Pure & Appl. Chem., Vol. 70, No. 11, pp. 2189–2200, 1998.
Printed in Great Britain.

Mimicking bacterial photosynthesis

Devens Gust, Thomas A. Moore and Ana L. Moore

Department of Chemistry and Biochemistry and Center for the Study of Early Events in Photosynthesis, Arizona State University, Tempe, AZ 85287-1604

Abstract: Photosynthesis in bacteria involves absorption of light by antenna chromophores and transfer of excitation to reaction centers, which convert the excitation energy to electrochemical potential energy in the form of transmembrane charge separation. A proton pump uses this stored energy to generate proton motive force across the membrane, which in turn is used to synthesize adenosine triphosphate (ATP). All of these steps can now be mimicked in the laboratory. Artificial antennas and reaction centers can be prepared from chromophores, electron donors and electron acceptors linked by covalent bonds. The artificial reaction centers can be inserted into the lipid bilayers of liposomes, where they act as constituents of transmembrane light-driven proton pumps. Finally, the proton gradient thus produced can be used to synthesize ATP via catalysis by F_0F_1-ATP synthase isolated from chloroplasts. The synthetic and natural systems can use light energy to produce ATP at comparable chemical potentials.

INTRODUCTION

The impetus underlying much photochemical research has long been the possibility of mimicking the process by which photosynthetic organisms harvest sunlight and convert its energy to more useful forms (1). There are myriad promising approaches to this problem that use materials and principles from many areas of chemistry and biology. In this paper we will describe one approach, which has been explored in our laboratories for about 20 years and which has allowed mimicry of all of the basic steps of natural solar energy conversion.

As a model, we have taken photosynthesis in purple non-sulfur photosynthetic bacteria. The process in these bacteria has much in common with green plant photosynthesis, but is simpler and better understood. We will briefly describe this natural energy conversion sequence, and then illustrate how it can be mimicked. The bacterial process is illustrated diagrammatically in Fig. 1. Photosynthesis is a transmembrane process, and the major components are housed in and span the lipid bilayer of the bacterial cell membrane. Sunlight is absorbed by an antenna system that contains chromophores such as bacteriochlorophyll and carotenoid polyenes. A variety of chromophores and protein environments is used so that light can be efficiently absorbed throughout the solar

*Lecture presented at the 17th IUPAC Symposium on Photochemistry, Sitges, Barcelona, Spain, 19–24 July 1998. Other presentations are published in this issue, pp. 2147–2232.

spectrum. Singlet excitation energy is rapidly transferred among the antenna chromophores, and ultimately to the reaction center. The role of the reaction center is to convert excitation energy to electrochemical energy in the form of transmembrane charge separation. The first step is photoinduced electron transfer from a special pair of bacteriochlorophylls via an accessory bacteriochlorophyll to a bacteriopheophytin molecule. Next, an electron migrates from the bacteriopheophytin to a quinone Q_A, and then on to a second quinone Q_B. After reduction of the oxidized special pair by a *c*-type cytochrome, the energy of a second photon is used to transfer a second electron to Q_B. The resulting hydroquinone diffuses to the cytochrome bc_1 complex, which is a transmembrane proton pump. It reoxidizes the hydroquinone back to a quinone and uses the resulting reduction potential, via the *c*-type cytochrome, to reduce the special pair, thus regenerating the reaction center. The energy released is used to transfer protons across the membrane, establishing a proton motive force across the bilayer. Finally, protons flow back across the membrane in the direction of the proton gradient and the energy produced drives the synthesis of adenosine triphosphate (ATP) from adenosine diphosphate (ADP) and inorganic phosphate (Pi) with catalysis by ATP synthase. Thus, the overall photosynthetic process uses light energy to produce ATP at high chemical potential, and the resulting high-energy phosphate is used to fill the various energy needs of the organism.

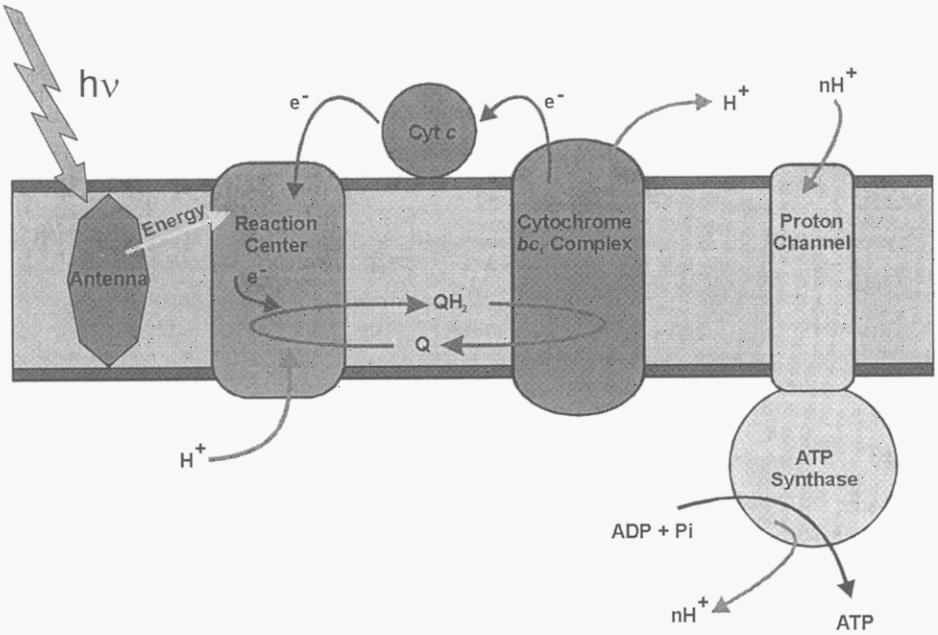

Fig. 1. Schematic representation of the photosynthetic apparatus of purple bacteria.

Although the major components of the bacterial photosynthetic apparatus are proteins, the photochemical aspects of energy conversion are all carried out by organic chromophores and other cofactors. This suggests a strategy for mimicry of the early steps of photosynthesis: construct artificial systems based on chromophores, electron donors and electron acceptors related to those found in the natural system, but replace the organizational role of the protein with some other organizational principle. In our work, we have used covalent linkages to control the separations, mutual orientations, and electronic coupling interactions between molecules that in turn control the rates and yields of energy and electron transfer reactions (2-5). How can we apply this strategy, and how close can we come to mimicry of the natural process? The state of the art in our laboratories is illustrated below.

MIMICKING ANTENNA FUNCTION

The minimum requirements for a simple synthetic system that can mimic the basic singlet energy transfer processes of photosynthesis are a light-absorbing excitation donor, an energy-accepting chromophore, and sufficient electronic interaction such that singlet-singlet energy transfer is more rapid than depopulation of the donor excited singlet state by other pathways such as internal conversion, intersystem crossing, and fluorescence. Porphyrin dyad **1** meets these criteria (6). It consists of a zinc tetraarylporphyrin (P_{Zn}) linked to a free base porphyrin (P) by an amide bond. The energy of the first excited singlet state of the zinc porphyrin is 2.08 eV, whereas that of the free base porphyrin is 1.90 eV. Thus, absorption of light by the zinc porphyrin followed by singlet-singlet energy transfer to the free base is energetically favorable. In fact, excitation of this dyad in dichloromethane solution at 550 nm, where both porphyrin moieties absorb light, yields a fluorescence emission spectrum that features significant emission only from the free base porphyrin. The zinc porphyrin excited singlet state is strongly quenched. The fluorescence excitation spectrum for emission by the free base porphyrin shows that this quenching is due to singlet-singlet energy transfer from $^1P_{Zn}$ to P that occurs with a quantum yield of 0.97. The zinc porphyrin acts as an antenna for the free base. The rate constant for singlet-singlet energy transfer, 2.3×10^{10} s^{-1}, was obtained from time-resolved emission studies, in which the zinc porphyrin fluorescence decayed at the same rate that the free base emission grew in. Singlet-singlet energy transfer in linked donor-acceptor systems is relatively easy to achieve, and many examples may be found in the literature. The same principles may be used to design complicated antenna systems in which many chromophores funnel excitation to an energy sink, where it is potentially available for useful purposes.

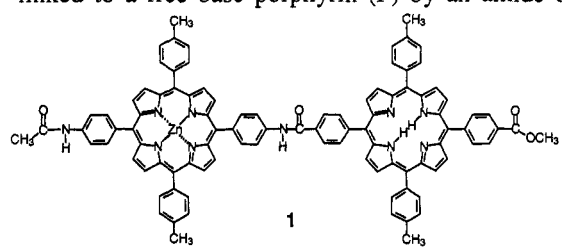

1

REACTION CENTER MIMICS

The reaction center is basically a transmembrane molecular-scale photovoltaic device. It uses light energy to transfer an electron across the thickness of the bilayer. Thus, the

underlying photochemical principle is photoinduced electron transfer. The most basic reaction center mimic must contain a chromophore that can act as an excited state electron donor (or acceptor) and an electron acceptor (donor) moiety with a suitable reduction (oxidation) potential. These species must have sufficient electronic coupling so that photoinduced electron transfer is rapid enough to compete with decay of the excited state by other pathways.

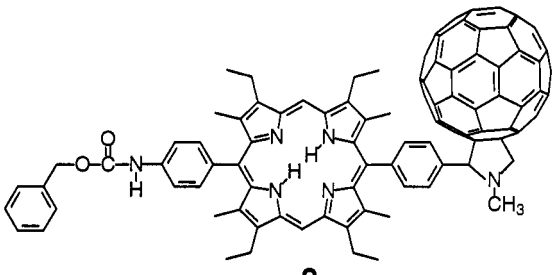

2

Porphyrin-fullerene (P-C_{60}) dyad **2** is an example of such a system (7). The porphyrin serves as an electron donor chromophore and chlorophyll model, whereas fullerenes have proven to be excellent electron acceptors in such applications (8-10). Excitation of this dyad in benzonitrile solution with a 200-fs laser pulse at 590 nm leads to the observation of the transient absorption spectra shown in Fig. 2 (11). These spectra contain features characteristic of the fullerene radical anion (absorption in the 1000-nm region) and the porphyrin radical cation (absorption in the 600 – 700 nm region). Excitation at 590 nm generates mainly the porphyrin first excited singlet state, ^{1}P-C_{60}. Fig. 2 shows that the porphyrin first excited singlet state rapidly transfers an electron to the fullerene to generate the $P^{\bullet+}$-$C_{60}^{\bullet-}$ charge-separated state. Studies of the time evolution of the transient spectrum show that ^{1}P-C_{60} forms with the excitation pulse and transfers an electron to the fullerene with a rate constant of 8.1×10^{10} s^{-1}, giving $P^{\bullet+}$-$C_{60}^{\bullet-}$ with a quantum yield of essentially 1.0. The charge-separated state undergoes recombinaton with a rate constant of 1.5×10^{10} s^{-1}.

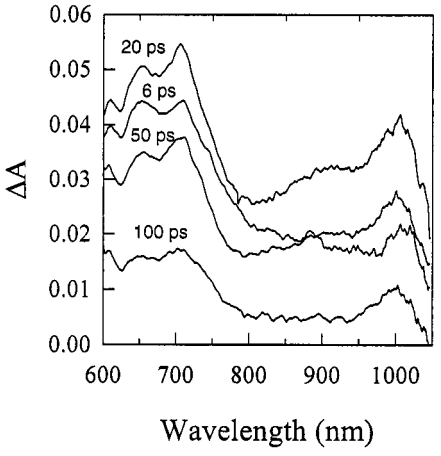

Fig. 2. Transient absorption spectra for dyad **2** in benzonitrile following excitation with a 590 nm, 200 fs, 20 μJ laser pulse.

The results for **2** show that in many ways, this dyad is a good model for electron transfer in natural reaction centers. The porphyrin excited singlet state undergoes photoinduced electron transfer to generate the charge-separated state with a quantum yield of unity, and this state preserves about 1.4 eV of the 2.0 eV inherent in the porphyrin excited singlet state. However, this dyad, in common with other two-component donor-acceptor systems, suffers from a short lifetime for the charge-separated state. The charge-

separation lifetime on the picosecond time scale prevents facile access to the stored energy via subsequent chemical reactions, and the stored energy is simply lost as heat. The photosynthetic reaction center circumvents this problem by using a multistep electron transfer strategy. The radical cation and anion are separated by a series of electron transfer steps, each of which is short-range, rapid and efficient. The result is a state in which the charges are spatially and electronically isolated, so that charge recombination is slow. Some time ago, we first applied this strategy to the design of artificial reaction centers (12,13). Molecular triad **3** illustrates the idea (7).

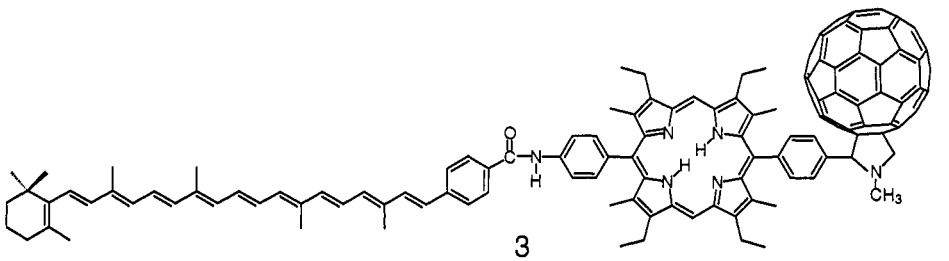

3

The triad consists of a porphyrin-fullerene system such as that in **2** with the addition of a carotenoid polyene (C), which acts as a secondary electron donor. The photochemistry of the triad is illustrated in Fig. 3. The energetics in the figure are based on spectroscopic and cyclic voltammetric measurements in polar solvents. Excitation of the porphyrin moiety of **3** leads to C-^{1}P-C_{60}, which decays by photoinduced electron transfer step 3, as in dyad **2**, to give C-$P^{\bullet+}$-$C_{60}^{\bullet-}$ with a quantum yield of unity. This charge-separated state may recombine by step 7 to give the ground electronic state, as in the dyad. However, competing with charge recombination is a second electron transfer from the carotenoid to the porphyrin radical cation (step 4), yielding a final $C^{\bullet+}$-P-$C_{60}^{\bullet-}$ charge-separated state. In the final state, the radicals are separated by the neutral porphyrin moiety, and therefore charge recombination might be expected to be slow relative to that in dyad **2**. In fact, as illustrated in Fig. 4, the lifetime of $C^{\bullet+}$-

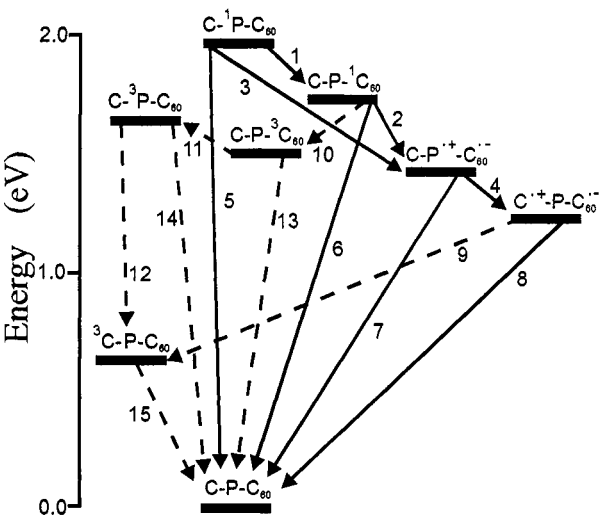

Fig. 3. High energy states of C-P-C_{60} triad **3** and relevant interconversion pathways.

$P\text{-}C_{60}^{\bullet-}$ is 770 ns in benzonitrile and 170 ns in 2-methyltetrahydrofuran. The quantum yield is 0.12 in benzonitrile and 0.14 in 2-methyltetrahydrofuran, as determined by the comparative method.

In triad **3**, the multistep electron transfer sequence increases the lifetime of the charge-separated state by a factor of over 10,000, providing time for potentially harvesting the stored energy by diffusional or other chemical or electrical processes. The price paid for this extension is a lower amount of stored energy, and, in this case, a lower overall quantum yield of charge separation. In other model reaction centers we have studied, the quantum yield of the final state approaches unity (5).

The photochemistry of triad **3** has several other features that are reminiscent of photosynthetic electron transfer. In the first place, the charge recombination of $C^{\bullet+}\text{-}P\text{-}C_{60}^{\bullet-}$ shown in Fig. 4 does not yield the ground state, but rather the carotenoid triplet state, $^3C\text{-}P\text{-}C_{60}$. This triplet formation by the radical pair mechanism involves evolution of the initially formed singlet biradical into the triplet biradical, which then recombines to yield the carotenoid spectroscopic triplet, as confirmed by epr spectroscopy (14). Such recombination is unusual in model systems, but has been observed in natural photosynthetic reaction centers. In addition, photoinduced electron transfer to form $C^{\bullet+}\text{-}P\text{-}C_{60}^{\bullet-}$ is observed in a frozen 2-methyltetrahydrofuran glass down to at least 8 K. The lifetime of the final state is 1.5 μs at 77 K, and charge recombination again yields the carotenoid triplet state. In bacterial reaction centers, photoinduced electron transfer occurs even at 4 K. In most model reaction centers, however, electron transfer ceases when the solvent becomes glassy due to destabilization of the charge-separated state by the frozen solvent, whose molecules are no longer able to reorient in order to stabilize the radical ions. These two unusual features of photoinduced electron transfer in the fullerene-based model reaction center may be ascribed at least in part to a much reduced sensitivity of the fullerene component to solvent effects on the energy of the radical anion and a smaller reorganization energy for electron transfer, relative to more common electron acceptor moieties such as quinones.

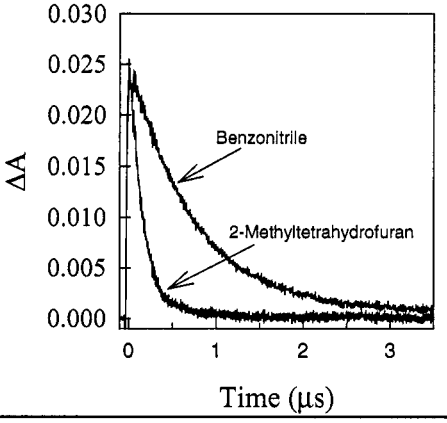

Fig. 4. Decay of the transient absorbance at 950 nm of triad **3** following laser excitation with a 5 ns, 590 nm laser pulse.

TRANSMEMBRANE PROTON PUMPING

The accessibility of artificial photosynthetic reaction centers makes it possible to take the next step in the mimicry of bacterial photosynthesis: conversion of light energy to proton motive force. This has now been achieved using triad-type artificial reaction centers (15).

The membrane component consists of liposomes prepared by the reverse-phase evaporation method from a 2:3 mixture of phosphatidylserine and dioleoylphosphatidylcholine. The average diameter of liposomes of this type is 100 nm.

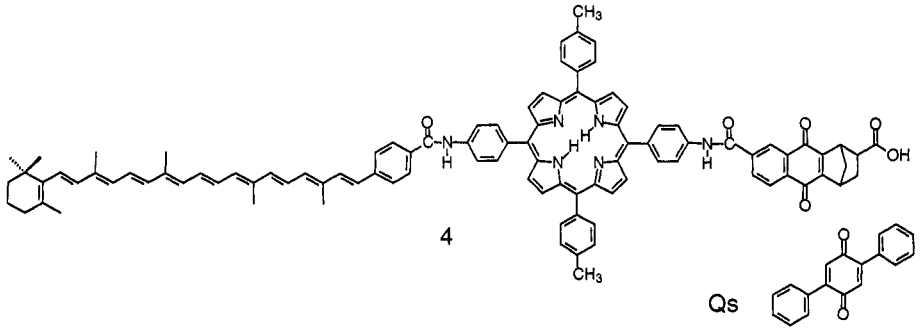

The liposome bilayers also contained the lipid-soluble 2,5-diphenylbenzoquinone, Q_s. To a solution of these liposomes in 0.05 M aqueous KCl was added carotene-porphyrin-quinone (C-P-Q) triad **4** in tetrahydrofuran. Upon dissipation of the organic solvent, the triad molecules, which are not soluble in water, insert into the liposome bilayer. It will be noted that the quinone portion of the triad bears a carboxylic acid group, which is ionized under the conditions of the experiment. The carotenoid portion of the molecule is extremely lipophilic. Thus, the triads would be expected to insert into the membrane with the quinone portion near the external aqueous interface and the carotenoid buried within the bilayer, as suggested schematically in Fig. 5. Laser flash photolysis experiments using a water-soluble reducing agent support this proposed preferential orientation of the triad molecules in the bilayer.

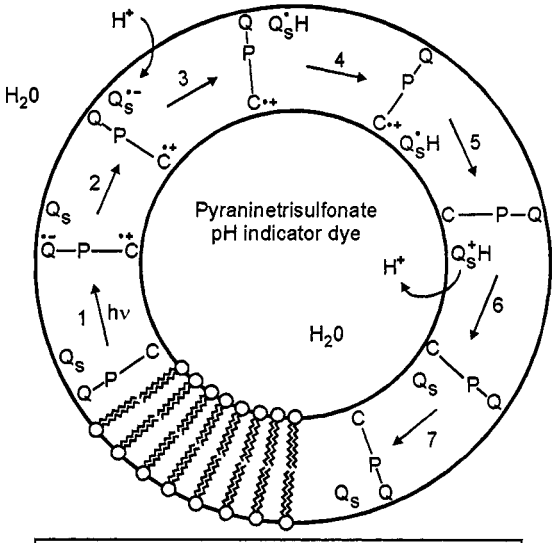

Fig. 5. Schematic representation of the liposome-based light-driven proton pump. The chemical structures of the components are shown above.

The vectorially-oriented triad and the quinone Q_s are the components of a light-driven proton pump that can transport protons across the lipid membrane and into the liposome interior. The import of protons into the liposome was monitored by the water-soluble dye pyraninetrisulfonate, which was placed in the aqueous environment inside the liposome. The first step

of the experiment consists of excitation of the liposome system with 650-nm light, which is absorbed only by the triad molecules. After some minutes of illumination, the light is turned off, and the exciation spectrum of the pyraninetrisulfonate fluorescence is measured. The change in protonation state of the dye, reflecting of the number of protons transported into the liposome, is determined by the ratio of fluorescence intensities for excitation of the protonated (406 nm) and nonprotonated (456 nm) forms of the dye. Fig. 6 shows typical results for such an experiment. The increasing ratio I_{406}/I_{456} with irradiation time indicates that the dye population is increasingly shifted toward the protonated form as a result of light-driven proton transport from the outside to the inside of the liposomes.

A proposed mechanism for this proton translocation may be discussed with reference to Fig. 5. Excitation of the triad generates the $C^{\bullet+}$-P-$Q^{\bullet-}$ charge-separated state via the type of photochemistry illustrated for triad **3**. The charge-separated state in the bilayer can be detected using transient absorption spectroscopy by observing the carotenoid radical cation absorbance in the 930-nm region. The quinone Q_s is more easily reduced than the naphthoquinone on the triad, and therefore accepts an electron from the charge-separated state to generate the Q_s radical anion, which is basic enough to accept a proton from the nearby external aqueous phase. The resulting neutral semiquinone is lipid soluble, and diffuses within the lipophilic part of the bilayer. When it encounters a carotenoid radical cation near the internal aqueous phase, it is readily oxidized, yielding a protonated quinone, Q_sH^+. This strong acid releases a proton to the nearby interior aqueous volume, thereby lowering the pH inside the liposome and regenerating the components of the proton pump. The specific details of the proton-pumping photocycle may differ somewhat from this simple picture, but Fig. 5 describes the basic features of the system.

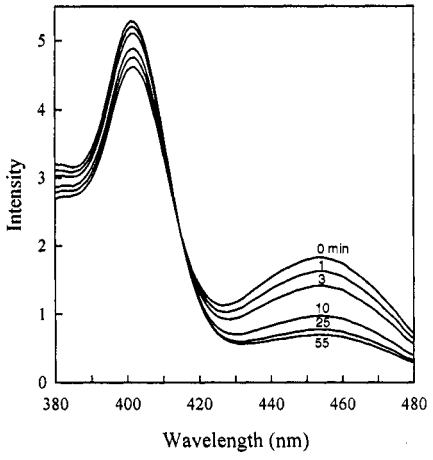

Fig. 6 Excitation spectra for emission at 510 nm of pyraninetrisulfonate inside liposomes containing **4** and Q_s. The liposomes had been illuminated with 650-nm light for the times indicated.

Control experiments are consistent with the proposed mechanism. No proton transport was observed if the solution was kept in the dark, or illuminated at 780 nm where the triad does not absorb. Liposomes lacking the shuttle quinone Q_s or triad **4** did not exhibit proton pumping. Prereduction of the quinone moieties with sodium dithionite also abolished the effect. Finally, addition of the proton ionophore carbonyl cyanide 4-(trifluoromethoxyphenylhydrazone) (FCCP) to the system after establishment of a proton gradient was found to relax the protonation state of the dye to its level prior to irradiation. Thus, mimicry of the third stage of bacterial photosynthesis, light-driven transmembrane proton pumping, has been achieved.

ATP SYNTHESIS

Proton motive force is a basic form of biological energy that is used to drive most energy-requiring reactions in living organisms. In photosynthetic bacteria, it is used to power the synthesis of ATP. Having prepared a light-driven transmembrane proton pumping system, we have attempted to use it to power ATP synthesis in a biomimetic fashion. In nature, ATP is synthesized by enzymatic systems that span the lipid bilayer. Protons are allowed to pass through the enzyme from one side of the membrane to the other in the direction of the pH gradient, and the energy provided by relaxation of the electrochemical potential gradient is used to synthesize ATP from ADP and Pi.

Conditions for extraction of the CF_0F_1-ATP synthase from spinach chloroplast thylakoids and reconstitution of the functional enzyme into liposomes have been developed. Using this methodology, the enzyme has been reconstituted into liposomes containing the components of the light-driven proton pump discussed above (16).

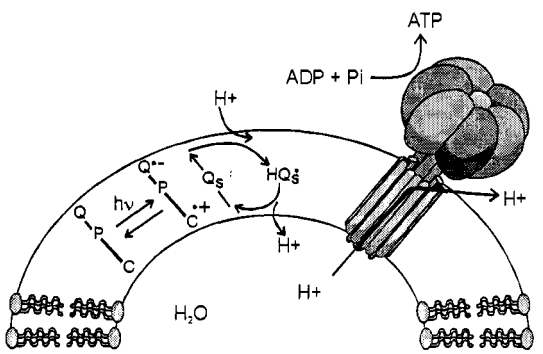

Fig. 7 A liposome-based artificial photosynthetic membrane for the light-driven synthesis of ATP.

The system is diagrammed in Fig. 7. The liposomes were formed from a 10:1 mixture of egg phosphatidylcholine and egg phosphatidic acid containing 20% cholesterol. The ATP synthase was inserted into the bilayer with the ATP-synthesizing portion of the enzyme extending out into the external aqueous solution. The constituents of the proton pump were incorporated as described above. Thioredoxin (10 μM) was added to activate the enzyme, and ADP, Pi and an initial amount of ATP were added to the external phase. The aqueous phases were adjusted to a pH of 8 prior to illumination. The liposomes were illuminated for various periods of time with laser light at 633 nm, which was absorbed only by the triad. Illumination was terminated, and the ATP produced was measured using a calibrated luciferin/luciferase assay, which is based on the luminescence of oxyluciferin.

The results of a typical experiment are shown in Fig. 8. In this experiment, the ATP concentration prior to illumination was ~2×10^{-7} M, and the ADP concentration was ~1000 times larger. The figure shows the oxyluciferin luminescence spectrum recorded as a function of illumination time. The increase in luminescence with exposure to actinic light is clear evidence of an increase in ATP concentration with illumination.

In order to establish that this increase was indeed due to ATP synthesis driven by light-induced proton motive force, several control experiments were performed. As shown in Fig. 9, no ATP was synthesized when 1 μM FCCP, the proton ionophore mentioned

above, was added to the system, making the membrane permeable to protons. Addition of 2 μM tentoxin, which is a specific inhibitor of CF_0F_1-ATP synthase, halted ATP synthesis, as did omission of the shuttle quinone Q_s or ADP. Likewise, omission of Pi, triad **4**, or ATP synthase abolished the effect.

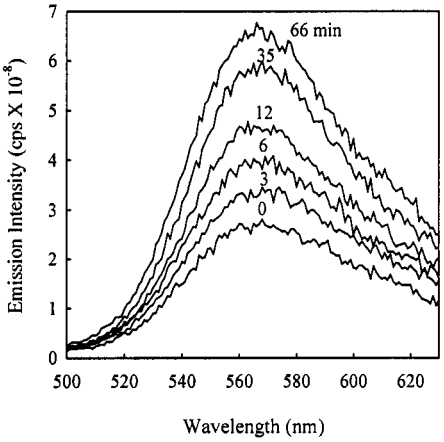

Fig. 8. Production of ATP by the liposome system as measured by the luciferin/luciferase assay after illumination with a 5 mW beam of light at 633 nm for the times shown.

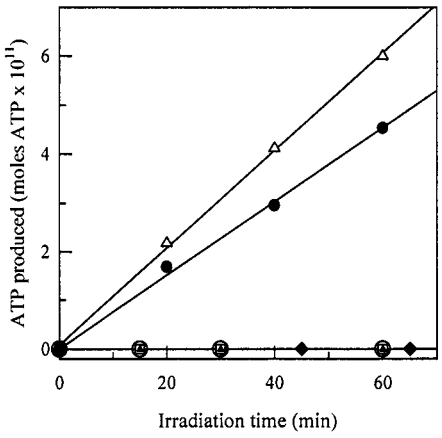

Fig. 9. Synthesis of ATP at [ATP] = [ADP] = 0.2 mM and [Pi] = 5 mM (△), and [ATP] = 0.2 mM, [ADP] = 0.02 mM, and [Pi] = 5 mM (●). Also shown are the results of control experiments discussed in the text.

At low levels of illumination, where ATP synthesis was limited by light absorption, it was found that one ATP molecule was synthesized for every 14 photons incident on the sample. As approximately 50% of the light was absorbed by the scattering liposome solutions, this corresponds to a quantum yield of ~0.15. Assuming that four protons must be transported out of the liposome by ATP synthase per molecule of ATP produced, the yield of the proton pump must be ~0.6. It should be noted that the liposomes used for ATP synthesis were of a different size and lipid mix from those used in the proton translocation experiments discussed in the previous section, and that approximately 1000 triad **4** molecules could be incorporated into one proteoliposome. In the proton translocation experiments, only ~40 triad molecules were present in each liposome.

In order to determine the turnover number of the system, the enzyme was saturated with ADP and Pi, and the system was operated under conditions of light saturation of ATP synthesis (~10 $mWcm^{-2}$). For maximum activity, non-catalytic ATP binding sites on the ATP synthase must be occupied. This was assured by adding 0.2 mM ATP before irradiation. Under these conditions, the turnover number was 7 ± 1 ATP per CF_0F_1-ATP synthase per second. This number is higher than has been reported for hybrid systems

using preparations of natural photosystem I as the proton pump, and similar to that observed in bacteriorhodopsin/ATP synthase constructs. It is likely that the turnover is limited by kinetic constraints in the photocyclic proton pump.

As illustrated in Fig. 9, the liposome system can synthesize ATP against a considerable ATP chemical potential. Under the conditions of 0.2 mM ATP, 0.02 mM ADP and 5 mM Pi shown in Fig. 9, ATP is synthesized against a chemical potential of ~12 kcal/mol. Thus, the system is converting light energy to chemical potential, rather than simply catalyzing an exergonic reaction. Based on the ATP potential, the quantum yield and the energy of 633-nm photons, we estimate that ~4% of the absorbed light energy is conserved in the system. The limits of the system have not as yet been reached, nor has the system been optimized.

CONCLUSIONS

As briefly described in this article, it is now possible to mimic the basic features of bacterial photosynthetic solar energy conversion in a mostly artificial, "bionic" construct. Light energy may be harvested by artificial antenna chromophores and transported to artificial reaction centers, where it initiates electron transfer reactions. Temporal stabilization of the resulting charge-separated states using a multistep electron transfer strategy permits harvesting of the stored energy before it is lost as heat. The stored energy may be used to transport protons across a lipid bilayer, generating a proton motive force which in turn may be used to drive ATP synthesis. Optimization of these systems should provide solar biological "power packs" that could be used to drive the enzymatic synthesis of other high-energy or high-value compounds, or power natural or artificial nanoscale "machines." Both scientific and practical uses of such modules can be easily envisioned.

ACKNOWLEDGMENT

The authors gratefully acknowledge the contributions of the students, colleagues and collaborators who helped carry out this research and who are listed as authors of the cited references. This work was supported by grants from the Office of Basic Energy Sciences, U. S. Department of Energy (DE-FG03-93ER14404) and the National Science Foundation (CHE-9709272).

REFERENCES

1. G. Ciamician. *Science* 36, 385-394 (1912).
2. D. Gust, T. A. Moore. *Science* 244, 35-41 (1989).
3. D. Gust, T. A. Moore. *Top. Curr. Chem.* 159, 103-151 (1991).
4. D. Gust, T. A. Moore. *Adv. Photochem.* 16, 1-65 (1991).
5. D. Gust, T. A. Moore, A. L. Moore. *Acc. Chem. Res.* 26, 198-205 (1993).
6. D. Gust, T. A. Moore, A. L. Moore, F. Gao, D. Luttrull, J. M. DeGraziano, X. C. Ma, L. R. Makings, S.-J. Lee, T. T. Trier, E. Bittersmann, G. R. Seely, S. Woodward, R. V. Bensasson, M. Rougée, F. C. de Schryver, M. Van der Auweraer. *J. Am. Chem. Soc.* 113, 3638-3649 (1991).

7. P. A. Liddell, D. Kuciauskas, J. P. Sumida, B. Nash, D. Nguyen, A. L. Moore, T. A. Moore, D. Gust. *J. Am. Chem. Soc.* 119, 1400-1405 (1997).
8. H. Imahori, S. Cardoso, D. Tatman, S. Lin, A. N. Macpherson, L. Noss, G. R. Seely, L. Sereno, J. Chessa de Silber, T. A. Moore, A. L. Moore, D. Gust. *Photochem. Photobiol.* 62, 1009-1014 (1995).
9. D. Kuciauskas, S. Lin, G. R. Seely, A. L. Moore, T. A. Moore, D. Gust, T. Drovetskaya, C. A. Reed, P. D. W. Boyd. *J. Phys. Chem.* 100, 15926-15932 (1996).
10. P. A. Liddell, J. P. Sumida, A. N. Macpherson, L. Noss, G. R. Seely, K. N. Clark, A. L. Moore, T. A. Moore, D. Gust. *Photochem. Photobiol.* 60, 537-541 (1994).
11. D. Gust, T. A. Moore, A. L. Moore, P. A. Liddell, D. Kuciauskas, J. P. Sumida, B. Nash, D. Nguyen. In *Recent Advances in the Chemistry and Physics of Fullerenes and Related Materials, Vol. 4,* (K. M. Kadish and R. S. Ruoff, eds.), The Electrochemical Society, Pennington, NJ, pp. 9-24 (1997).
12. D. Gust, P. Mathis, A. L. Moore, P. A. Liddell, G. A. Nemeth, W. R. Lehman, T. A. Moore, R. V. Bensasson, E. J. Land, C. Chachaty. *Photochem. Photobiol.* 37S, 46-46 (1983).
13. T. A. Moore, D. Gust, P. Mathis, J.-C. Mialocq, C. Chachaty, R. V. Bensasson, E. J. Land, D. Doizi, P. A. Liddell, W. R. Lehman, G. A. Nemeth, A. L. Moore. *Nature (London)* 307, 630-632 (1984).
14. D. Carbonera, M. Di Valentin, C. Corvaja, G. Agostini, G. Giacometti, P. A. Liddell, D. Kuciauskas, A. L. Moore, T. A. Moore, D. Gust *J. Am. Chem. Soc.* 120, 4398-4405 (1998).
15. G. Steinberg-Yfrach, P. A. Liddell, S.-C. Hung, A. L. Moore, D. Gust, T. A. Moore. *Nature (London)* 385, 239-241 (1997).
16. G. Steinberg-Yfrach, J.-L. Rigaud, E. N. Durantini, A. L. Moore, D. Gust, T. A. Moore. *Nature (London)* 392, 479-482 (1998).